Supplementary material for The hunt for the Kármán “constant” revisited

Peter A. Monkewitz and Hassan M. Nagib

May 11, 2023

1 Uncertainty analysis of S_0, κ and B_0 for the channel/duct experiments (Figure 3 of main paper)

The uncertainty of κ and S_0 for the channel experiments of figure 3 in the main text is estimated as follows. First the uncertainty of the linear slope S_0 is estimated as twice the standard deviation of $(\Xi - 1.1\,Y)$ between $y^+ = 600$ and $Y = 0.5$, which is a good measure of the width of the linear portion of Ξ_0 in figure 4a of the main text. The choice of the lower limit of $y^+ = 600$ for the estimate of the width of this linear portion is motivated by Monkewitz (2021), who noted the late start of the overlap in channel and pipe flow. At any rate, the influence of this choice on the following uncertainty estimates is weak. The resulting uncertainty of S_0 is $\pm 2\,\sigma = \pm\,0.406$, shown in figure 1. The uncertainties of κ and of the log-law constant B_0 are then determined as differences between the reference values $[\kappa, B_0] = [0.417, 5.5]$ for $S_0 = 1.1$ and the values of κ and B_0 for the modified $S_0 + 2\,\sigma = 1.506$, $S_0 - 1\,\sigma = 0.894$ and $S_0 - 2\,\sigma = 0.694$. They are obtained by minimizing the difference between U^+_∞, the mean velocity corrected for finite Reynolds number effects as in the main paper, and the sum of linear and logarithmic laws, i.e.

$$\Delta(S_0, B_0) = U^+_\infty - \{\frac{1}{\kappa}\ln \mathrm{Re}_\tau + S_0\,Y\} - \{\frac{1}{\kappa}\ln Y + B_0\} \qquad (1)$$

for each of the S_0 values.

Summary of uncertainty analysis for the channel/duct experiments

The estimate of $S_0 = 1.15$ was derived in section 2 of the main paper from channel DNS and has been slightly lowered to $S_0 = 1.1$ for the analysis of experimental channel/duct data. The resulting best fit $\kappa = 0.417$ is consistent

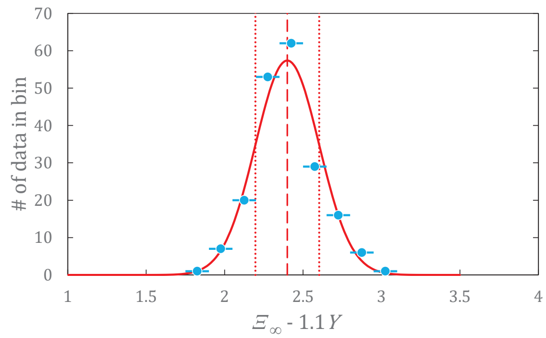

Figure 1: Analysis of the experimental channel data of figure 3 in the main text. Blue •, distribution of $(\Xi_\infty - 1.1Y)$ between $y^+ = 600$ and $Y = 0.5$ in bins of 0.15. Red —, fitted Gaussian distribution; - - -, mean of 2.40 ($\kappa = 1/2.40 = 0.417$); $\cdots$, mean $\pm\sigma$ ($\sigma = 0.203$).

with the value deduced from the mean velocity derivative of channel DNS in the main paper, but does not produce the optimal collapse in figures 2(c) and (d). With $S_0 = 0.897$, $\kappa = 0.405$ and $B_0 = 5.0$, the data collapse is seen to be improved in figure 4, suggesting that the optimal parameters for the channel/duct experiments considered are closer to $S_0 \approxeq 1$ and $\kappa \approxeq 0.41$.

1.1 Channel baseline case $S_0 = 1.1$

The baseline case considered here corresponds to figure 4 of the main text. To complement this figure, U_∞^+, corrected for finite Reynolds number effects, minus both linear part and log law (equation 1) is shown as figures 2c and 2d.

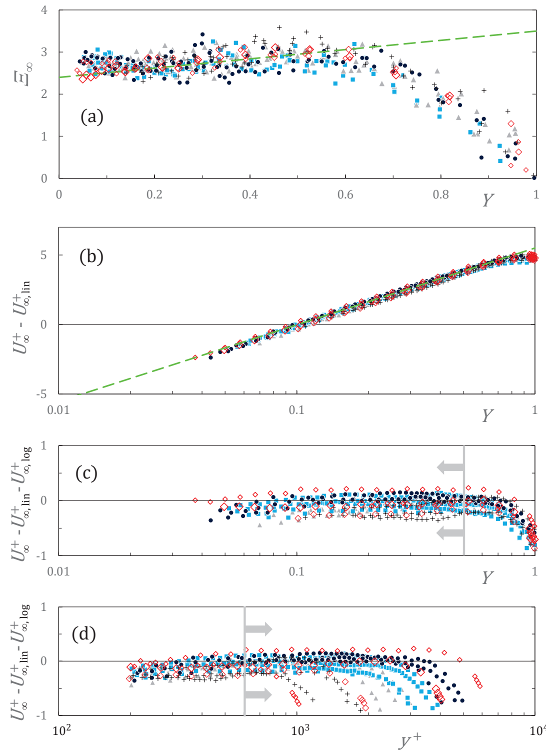

Figure 2: Baseline case of figure 3 in the main text with $S_0 = 1.1$ and $\kappa = 0.417$. (a): same as fig. 3a of main text. (b): same as fig. 3c of main text. (c): panel (b) minus log law, i.e. $U_\infty^+ - [(1/0.417)\ \ln \mathrm{Re}_\tau + 1.1\, Y] - [(1/0.417)\ \ln Y + 5.5]$; vertical grey line with arrows, upper limit $Y = 0.5$ of data used for the Gaussian distribution of figure 1. (d) Data of panel (c) versus y^+; vertical grey line with arrows, lower limit $y^+ = 600$ of data used for the Gaussian distribution of figure 1.

1.2 Channel with high value of $S_0 = 1.1 + 2\,\sigma = 1.506$

After changing S_0 to the high value of 1.506, κ and the log law constant B_0 are readjusted to minimize Δ in equation (1) over the largest possible interval of Y. This procedure yields $\kappa = 0.423$ and $B_0 = 5.6$

Note, that for this high value of S_0, the extent of the good fit of equation (1) is reduced from $Y \lessapprox 0.65$ for the baseline case of figure 2 to $Y \lessapprox 0.4$.

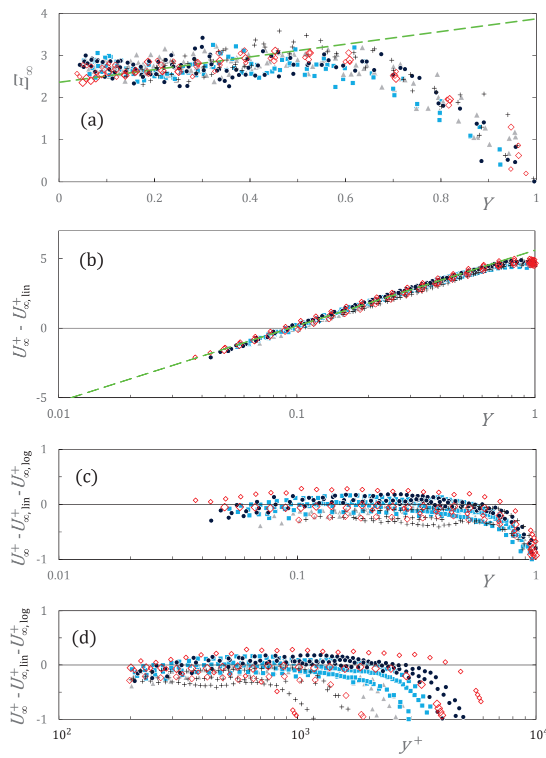

Figure 3: Analogous to figure 2 for the high slope $S_0 = 1.1 + 2\,\sigma = 1.506$, with the log law parameters adjusted to $\kappa = 0.423$ and $B_0 = 5.6$. Panels (c) and (d): $U_\infty^+ - [(1/0.423)\,\ln \mathrm{Re}_\tau + 1.506\,Y] - [(1/0.423)\,\ln Y + 5.6]$ versus Y and y^+.

1.3 Channel with moderately reduced value of $S_0 = 1.1 - 1\,\sigma = 0.897$

Using the same procedure as in section 1.2 for the moderately low value of $S_0 = 0.897$ results in $\kappa = 0.405$ and $B_0 = 5.0$, as shown in figure 4 below. For this value of S_0, the extent of the good fit of equation (1) extends to $Y \lessapprox 0.7$, similar to the baseline case of figure 2. More importantly, the data scatter is reduced relative to the baseline. Hence, the $\kappa = 0.417$, deduced from channel DNS in section 2 of the main paper, may be on the high side.

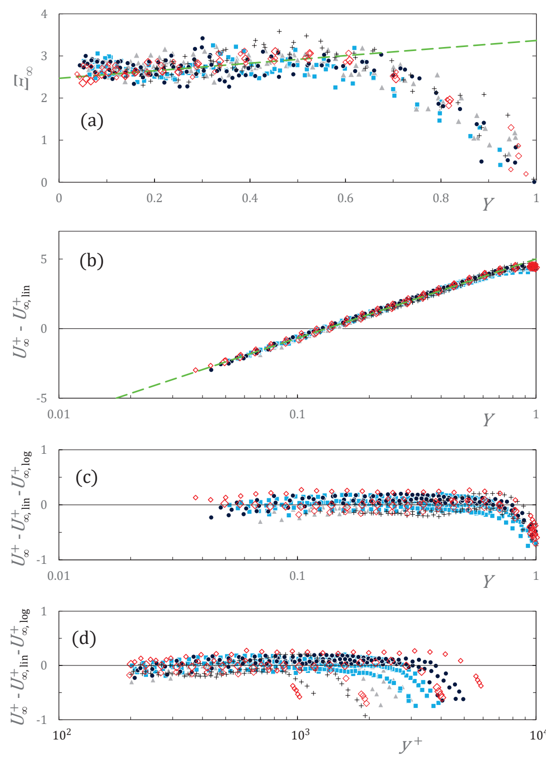

Figure 4: Analogous to figure 2 for the reduced slope $S_0 = 1.1 - 1\,\sigma = 0.897$, with the log law parameters adjusted to $\kappa = 0.405$ and $B_0 = 5.0$. Panels (c) and (d): $U_\infty^+ - [(1/0.405)\,\ln \mathrm{Re}_\tau + 0.897\,Y] - [(1/0.405)\,\ln Y + 5.0]$ versus Y and y^+.

1.4 Channel with strongly reduced value of $S_0 = 1.1 - 2\,\sigma = 0.694$

The same procedure as in sections 1.2 for the low value of $S_0 = 0.694$ results in $\kappa = 0.4$ and $B_0 = 4.9$, as shown in figure 5. For this low value of S_0, the fit in panels (c) and (d) appears to be not quite as good as in figure 4 above, but the Re_τ's are too low to allow a more precise determination of the optimal values for S_0, κ and B_0.

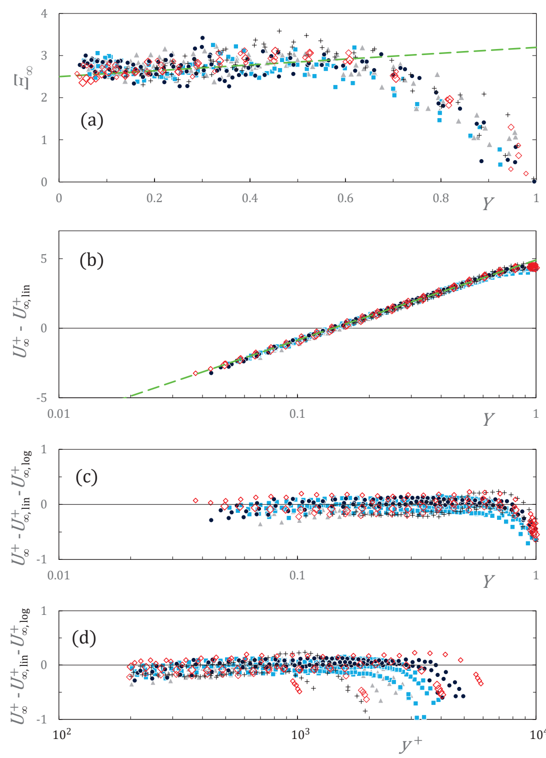

Figure 5: Analogous to figure 2 for the low slope $S_0 = 1.1 - 2\,\sigma = 0.694$, with the log law parameters adjusted to $\kappa = 0.400$ and $B_0 = 4.9$. Panels (c) and (d): $U_\infty^+ - [(1/0.400)\,\ln \mathrm{Re}_\tau + 0.694\,Y] - [(1/0.400)\,\ln Y + 4.9]$ versus Y and y^+.

2 Uncertainty analysis of S_0, κ and B_0 for the Superpipe experiment (Figure 5 of main paper)

The uncertainty of κ and S_0 for the Superpipe experiments of figure 5 in the main text is estimated as in section 1 for the channel.

First the uncertainty of the linear slope S_0 is "generously" estimated as twice the standard deviation of $(\Xi - 2.5\,Y)$ between $y^+ = 10^3$ and $Y = 0.5$, which is a good measure of the width of the linear portion of Ξ in figure 5a of the main text. The choice of the lower limit of $y^+ = 10^3$ for the estimate of the width of this linear portion is motivated by McKeon *et al.* (2004) and Monkewitz (2021), who noted the late start of the overlap in pipe flow. The resulting uncertainty of S_0 is $\pm 2\,\sigma = \pm\,0.544$, shown in figure 6.

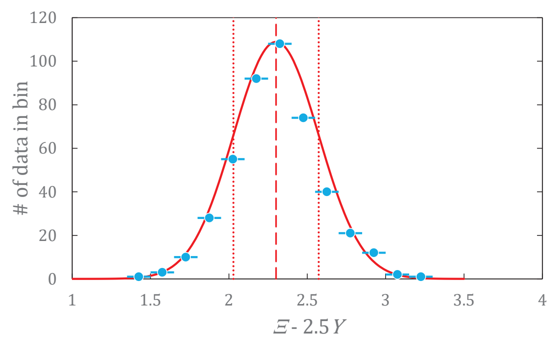

Figure 6: Analysis of the Superpipe data of figure 5 in the main text. Blue •, distribution of $\Xi_0 - 2.5Y$ between $y^+ = 10^3$ and $Y = 0.5$ in bins of 0.15 ($\mathrm{Re}_\tau = 5.3\,10^5$ not included in PDF). Red —, fitted Gaussian distribution; - - -, mean of 2.31 ($\kappa = 1/2.31 = 0.433$); $\cdots$, mean $\pm\sigma$ ($\sigma = 0.272$).

The uncertainties of κ and of the log-law constant B_0 are then determined as differences between the reference values $[\kappa, S_0] = [0.433, 5.9]$ for $S_0 = 2.5$ and the best fit values of κ and B_0 for the modified $S_0 \pm 2\,\sigma = 2.5 \pm\,0.544$, obtained by minimizing Δ in equation (1).

Summary of uncertainty analysis for the Superpipe experiment

As shown in section 3 of the main paper, the currently available pipe DNS do not yield a large variety of S_0 values. Therefore, the baseline value of $S_0 = 2.5$ was derived directly from the Superpipe data. Hence, $S_0 = 2.5$, $\kappa = 0.435$ and $B_0 = 5.9$ correspond to the optimal choice.

2.1 Pipe baseline case $S_0 = 2.5$

The baseline case corresponds to figure 6 of the main text. To complement this figure, U^+ minus the sum of linear part and log law (equation 1) is shown as figures 7c and 7d.

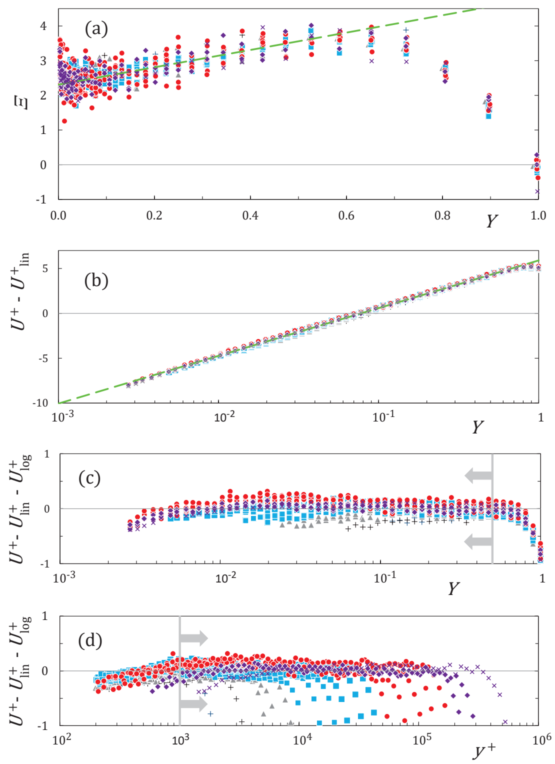

Figure 7: Baseline case of figure 5 in the main text with $S_0 = 2.5$ and $\kappa = 0.433$. (a): same as fig. 5a of main text. (b): same as fig. 6c of main text. (c): panel (b) minus log law, i.e. $U^+ - [(1/0.433)\ \ln \mathrm{Re}_\tau + 2.5\,Y] - [(1/0.433)\ \ln Y + 5.9]$; vertical grey line with arrows, upper limit $Y = 0.5$ of data used for the Gaussian distribution of the above figure 6. (d) Data of panel (c) versus y^+; vertical grey line with arrows, lower limit $y^+ = 10^3$ of data used for the Gaussian distribution of figure 6.

2.2 Pipe with high value of $S_0 = 2.5 + 2\,\sigma = 3.044$

After changing S_0 to the high value of 3.044, κ and the log law constant B_0 are readjusted until Δ in equation (1) is closest to zero over the largest possible interval of Y. This procedure yields $\kappa = 0.450$ and $B_0 = 6.6$
Note, that for this high value of S_0, the extent of the good fit of equation (1) is reduced from $Y \lessapprox 0.65$ for the baseline case of figure 7 to $Y \lessapprox 0.4$.

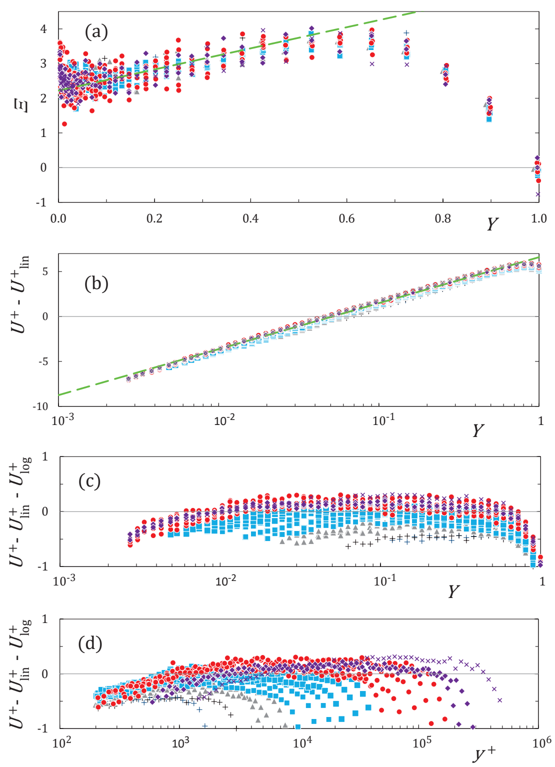

Figure 8: Analogous to figure 7 for the high slope $S_0 = 2.5 + 2\,\sigma = 3.044$, with the log law parameters adjusted to $\kappa = 0.45$ and $B_0 = 6.6$. Panels (c) and (d): $U^+ - [(1/0.45)\,\ln \mathrm{Re}_\tau + 3.044\,Y] - [(1/0.45)\,\ln Y + 6.6]$ versus Y and y^+.

2.3 Pipe with low value of $S_0 = 2.5 - 2\,\sigma = 1.956$

Using the same procedure as in section 2.2 for the low value of $S_0 = 1.956$ results in $\kappa = 0.425$ and $B_0 = 5.6$, as shown in figure 9 below. For this low value of S_0, the extent of near-zero Δ's in equation (1) increases to $Y \lessapprox 0.7$, similar to the baseline case of figure 7. However, the data in figure 9c are seen to have a positive "hump" beyond $Y \approx 0.3 - 0.4$. Therefore, even if the data scatter in figure 9 is somewhat reduced relative to figure 7, the baseline $\kappa = 0.435$ of figure 7 appears to be near the optimal fit. It also happens to be nearly equal to the original value given by Zagarola & Smits (1998)!

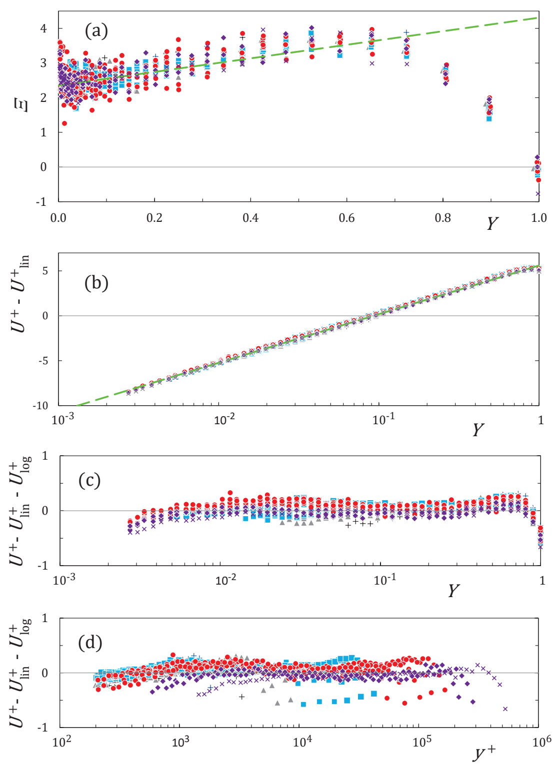

Figure 9: Analogous to figure 7 for the low slope $S_0 = 2.5 - 2\,\sigma = 1.956$, with the log law parameters adjusted to $\kappa = 0.425$ and $B_0 = 5.6$. Panels (c) and (d): $U^+ - [(1/0.425)\ \ln \mathrm{Re}_\tau + 1.956\,Y] - [(1/0.425)\ \ln Y + 5.6]$ versus Y and y^+.

References

McKeon, B. J., Li, J., Jiang, W., Morrison, J. F. & Smits, A. J. 2004 Further observations on the mean velocity distribution in fully developed pipe flow. *J. Fluid Mech.* **501**, 135–147.

Monkewitz, Peter A. 2021 The late start of the mean velocity overlap log law at $y^+ = \boldsymbol{O}(10^3)$ – a generic feature of turbulent wall layers in ducts. *Journal of Fluid Mechanics* **910**, A45 1–28.

Zagarola, M. V. & Smits, A. J. 1998 Mean-flow scaling of turbulent pipe flow. *J. Fluid Mech.* **373**, 33–79.